

Energy Feature of Air Bubble Detachment from a Low-Rank Coal Surface in the Presence of a Dodecane–Oleic Acid Collector Mixture

Maoyan An, Yinfei Liao,* Zhe Yang, Yijun Cao, Xiaodong Hao, Xingwei Song, Hourui Ren, Aosheng Yang, and Luojian Chen



Cite This: *ACS Omega* 2022, 7, 18315–18322



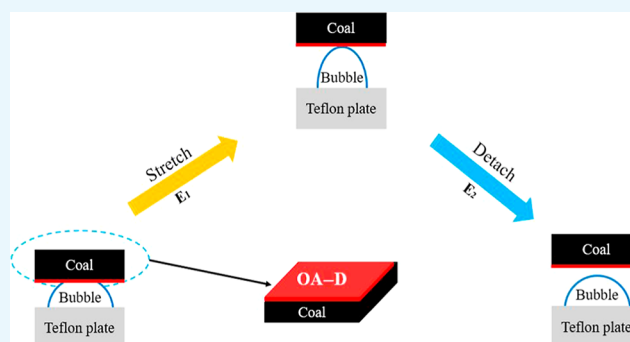
Read Online

ACCESS |

Metrics & More

Article Recommendations

ABSTRACT: It has been generally proved that mixed collectors can enhance the flotation of low-rank coal (LRC). However, the inhibition effect of mixed collectors on the detachment between particles and bubbles is still unclear. In this paper, the energy feature of air bubble detachment from the LRC surface in the presence of dodecane (D), oleic acid (OA), and the mixture of dodecane and oleic acid (OA–D) was studied. The effect of collectors on the LRC surface property was analyzed using contact angle measurement, X-ray photoelectron spectroscopy, and wetting heat measurement. The force and displacement during the detachment process were measured synchronously using microforce balance. The results showed that the collector treatment increased the C–C/C–H content and decreased the content of oxygen-containing groups on the LRC surface. The synergistic effect between OA and D enabled the mixed collector to exhibit higher contact angle and wetting heat. Bubble detachment from the LRC surface can be divided into two stages: bubble stretching and bubble sliding, which corresponded to activation energy and detachment work, respectively. The activation energy and detachment work decreased in the same order of OA–D > OA > D, indicating that the mixed collector OA–D increased the energy of bubble detachment from the LRC surface and enhanced the adhesion strength. The theoretical detachment work was calculated, and the calculated results were in agreement with the measured results. This research provides a new perspective on the mechanism of LRC flotation being improved by mixed collectors.



1. INTRODUCTION

China has abundant coal resources, among which low-rank coal (LRC) accounts for 50% of the total coal resources.^{1,2} It is of great significance to improve the product quality and beneficiation process, and comprehensively utilize the huge LRC reserves. Flotation is usually used for the separation of the LRC fines.³ The addition of common oily collectors, such as diesel oil, can significantly improve the surface hydrophobicity of particles, making it possible to separate clean coal and gangue.⁴ However, the surface of LRC has high porosity and abundant oxygen-containing functional groups, due to which the coal particles exhibit high hydrophilicity. The LRC property results in larger consumption of collectors and increases the difficulty of flotation.^{5,6}

Mixed collectors can achieve better separation performance than single collectors, which has been demonstrated by many researchers. Zhang et al.⁷ found that high clean yield and combustible material recovery was obtained in LRC flotation by using a mixed collector composed of nonpolar dodecane (D) and polar tetraethylene glycol monododecyl ether. When D was mixed with a small amount of THF (tetrahydrofurfuryl esters) as

the collector, the LRC surface hydrophobicity can be significantly improved.⁸ The addition of a certain amount of DTAC (dodecyl trimethyl ammonium chloride) in diesel oil can effectively enhance the LRC hydrophobicity and reduce the induction time between coal particles and bubbles.⁹

On the other hand, the adsorption behavior of the mixture of D and *n*-valeric acid on the LRC surface was revealed via molecular dynamics simulation.¹⁰ Due to the existence of *n*-valeric acid, the D molecules of the mixed collector were attracted and their movements were limited. This meant that the mobility of D molecules on the coal surface was reduced. Thus, the water molecules were accelerated to leave the LRC surface, which increased the lipophilicity and hydrophobicity of the LRC surface.¹⁰ A new synergistic mechanism of oleic acid–dodecane

Received: January 22, 2022

Accepted: May 17, 2022

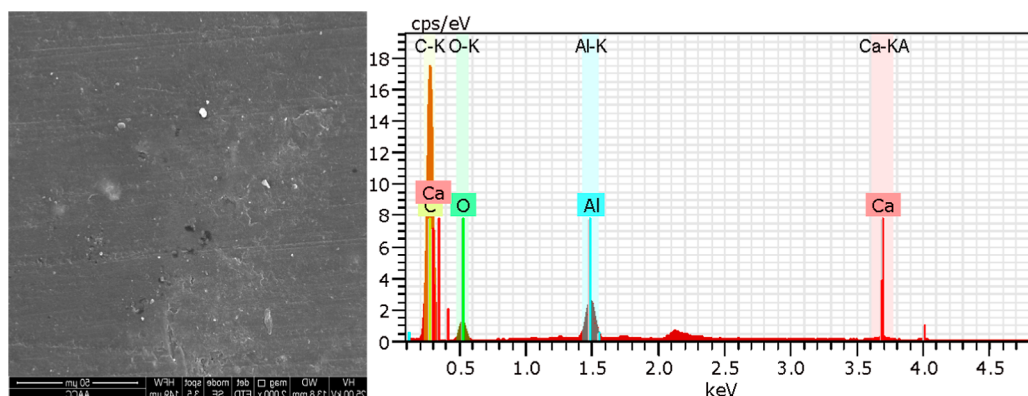
Published: May 25, 2022



Table 1. Proximate and Ultimate Analyses of the Coal Sample^a

substance	proximate analysis (%)				ultimate analyses (%)				
	Mad	Aad	Vadf	FCdaf	Hdaf	Cdaf	Ndaf	Std	Odaf
coal sample	3.37	5.62	37.53	62.48	5.08	79.20	1.06	0.30	14.03

^aad: air dry basis; daf: dry ash-free basis; and td: total content, dry ash-free basis.

**Figure 1.** Energy spectrum diagram of LRC particles.

(OA–D) mixed collectors was proposed by An et al.¹¹ On a relatively ordered “supramolecular structure” on the LRC surface, especially, there were hydrophobic and van der Waals forces between the OA chain and the D chain that can promote the formation of a continuous collector film. Although enhancing LRC flotation using a mixed collector has been widely studied, its effect on the bubble–particle detachment process is less-studied, especially the energy feature during the detachment process.

The interaction between bubbles and particles in the flotation process can be divided into three parts: collision, adsorption, and detachment.^{12,13} In the gas–liquid–solid three-phase flotation system, the target mineral particles collide and adhere to the bubbles and follow the bubbles up to the froth layer.¹² During the process of bubble–particle aggregation increase, some target mineral particles will detach from the bubble surface and fall off from the froth layer.¹⁴ Particle detachment is the main factor affecting flotation results that directly determines the recovery of useful minerals.¹⁴

As an important part of flotation, bubble–particle detachment has attracted wide attention. As early as 1960, Nutt studied the spherical particles adhering to the bubble, which were separated from the gas–liquid interface due to the centrifugal effect of the external flow field.¹⁵ He proposed that the force between the bubble and particles was composed of capillary force, buoyancy force, and centrifugal force, and the contact angle, surface tension, and liquid density affected the detachment force.¹⁵ Then, Schulze further studied the interaction between the bubble and particles and established a bubble–particle model to analyze the forces.¹⁶ Zhang et al.¹⁷ used a self-made bubble–particle separation measurement system to study the influence of vibration modes such as sine wave, triangular wave, and square wave vibration on the separation of LRC particles from vibrating bubbles, and the results showed that the agglomerate of bubble–particles was the most stable under sine wave vibration.

The collector has a considerable impact on the detachment of particles–bubbles, which can change the surface hydrophobicity of particles. The hydrophobicity of particles strongly influences the bubble–particle detachment force. The probability of the

detachment of particles from the bubbles is smaller if the particles are more hydrophobic.¹⁸ Fosu et al.¹⁹ studied the influence of the xanthate collector type and concentration on the detachment of coarse composite sphalerite particles from bubbles in flotation, and the results showed that the detachment of particles from oscillating bubble correlated well with the xanthate concentration and hydrocarbon chain length of xanthate ions. Wang et al.²⁰ proposed a methodology to characterize the collector strength by measuring the attachment rate of particles to a capillary-pinned bubble. This particle–bubble attachment method can be used to gain additional information not currently available from either contact angle measurements or bulk collector performance tests.

Some researchers reported that the detachment between particles and bubbles in coal flotation was significantly influenced by collectors.^{21,22} Zhu et al.²¹ used a new mixture of fossil oil and an oxygen-containing compound (FO) to enhance the flotation of LRC. It was indicated that when treated by FO, the coal particles had a lower probability of detachment from the bubble–particle aggregate because the critical amplitudes under different concentrations were the highest. Li et al.²² found that in the presence of shale oil, the surface of oxidized coal was more hydrophobic, more particles were attached to the surface of bubbles, and the detachment force between the particles and bubbles was greater. Chen et al.²³ investigated the effect of 2-ethylhexanol and didodecyltrimethylammonium bromide (DDAB) on the interaction between oily bubbles and coal particles, and they found that the detachment probability reduced with the increase of collector viscosity. Although the mixed collector is an effective collector for LRC flotation, its effect on the bubble–particle detachment is still unclear.

Our team has been committed to the study on the mechanism of mixed collectors to strengthen the LRC flotation.^{1,24–27} In our previous work, the detachment force of air bubbles detached from the LRC surface after collector treatment was studied,²⁸ In this paper, the energy feature of bubble detachment from the LRC surface in the presence of D, OA, and their mixture (OA–D) was investigated. The property of the coal samples was analyzed using X-ray photoelectron spectroscopy (XPS),

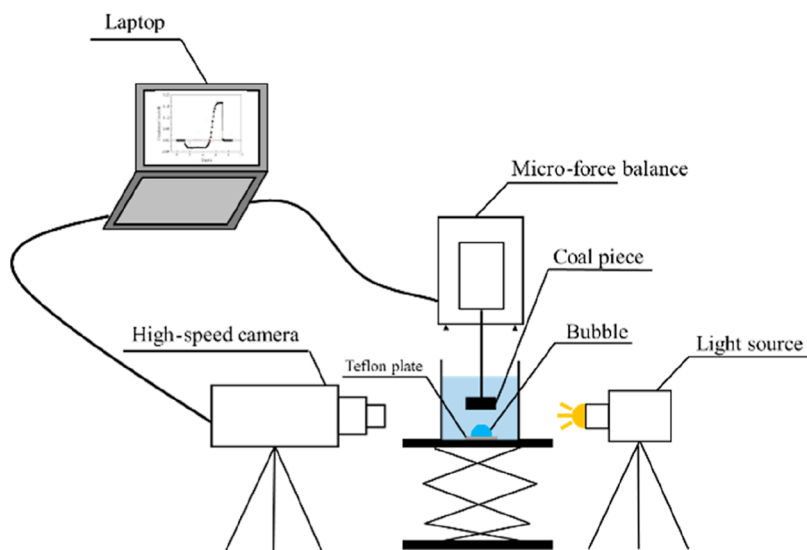


Figure 2. Force measure system for bubble detachment from the LRC surface.

scanning electron microscopy (SEM), contact angle measurement, and wetting heat measurement. The force and displacement of bubble detachment from the LRC surface treated by different collectors were measured using the microforce balance method. The effect of the mixed collector on the energy feature during the detachment process was discussed. The theoretical detachment energy was calculated based on the change of surface free energy. This study revealed the mechanism of the mixed collector enhancing LRC flotation from the perspective of detachment energy.

2. MATERIALS AND METHODS

2.1. Materials. The long flame coal sample was obtained from the Daliuta mine, Shanxi province, China. The coal sample was benefited by gravity separation, and then it was cut into pieces with the size of $40 \times 20 \times 15$ mm and polished using the sandpapers of 4000 grit. The proximate and ultimate analyses are shown in Table 1. The ash content (Aad) of the coal sample was relatively low, only 5.62%. However, the volatile matter content (Vdaf) was relatively high, up to 37.53%, and the oxygen content (Odaf) was 14.03%. This meant that the coal sample had a low metamorphic degree and a high degree of oxidation, which belonged to the typical LRC characteristics.

SEM (SU8200, HITACHI, Japan) was used to study the surface microstructure of the coal sample. The surface morphology of the LRC sample and the energy spectrum analysis are shown in Figure 1. The LRC sample had a relatively uniform and smooth surface. It can be seen that the content of C and O elements was high and there was only a small amount of Al and Ca in the LRC sample. The results indicated that the LRC sample possessed high purity with few impurities. Thus, it was suitable in studying the effect of the collector on bubble detachment from the LRC surface and reducing the experimental error.

2.2. Reagents. OA and *n*-dodecane were used as collectors and purchased from Aladdin chemical reagent company. The purity level of the chemicals was analytical purity. When the mass ratio of OA in the mixed collector was changed from 0.2 to 0.3, the interfacial tension between oil and water decreased by about 1.5 mN/m. In our previous work,^{1,29} the interfacial tension and flotation test reached good indexes at the ratio of

1:4. The price of OA was higher than that of common oil collectors, so the ratio between *n*-dodecane and OA was maintained to be 1:4 in this paper.

2.3. Methods. **2.3.1. Contact Angle Measurement.** The contact angle is a direct indicator that reflects the material surface wettability. The polished coal piece sample was immersed in different reagents for 3 h, and then, it was dried and placed in the DSA100 contact angle analyzer (Bruker, Germany). Finally, the sessile droplet method was used to measure the coal sample contact angle θ .

2.3.2. X-Ray Photoelectron Spectroscopy. XPS (ESCALAB 250Xi, Thermo Fisher, Waltham, MA, USA) measurement was used to analyze the adsorption of different reagents on the coal sample surface. A monochromatic aluminum anode target (Al $K\alpha$) was used as the radiation source with a spot size of $650 \mu\text{m}$. The pass energy was set at 20 eV, and the energy step size was set at 0.050 eV. The result was analyzed using Casa XPS software. The C 1s hydrocarbon peak was set at 284.6 eV to calibrate the C 1s binding energy.

2.3.3. Wetting Heat Measurement. The wet heat flow between the collectors and the coal sample was recorded via microcalorimetry using a C80 calorimeter (Setaram, Caluire, France). First, 8 mg of the coal sample and 2 mL of the collector were placed at the bottom and top of the cell, respectively. Then, the cell's firmware was installed and placed into the adiabatic chamber of the microcalorimeter. After the system was stabilized at 30 °C, the aluminum foil membrane was punctured to allow solid–liquid mixing. The dynamic wetting heat flow signal was recorded using data acquisition software in the calorimeter computer, and the wetting heat was finally obtained via integration of the wetting heat flow curve.

2.3.4. Energy Determination of Air Bubble Detachment from the LRC Surface. The mechanical test device used to study bubble detachment from the LRC surface is shown in Figure 2. The device was composed of a micro force balance, an electric lifting platform, a sample cell, a coal piece (suspended from a micro force balance sensor), a high-speed camera (I-speed 713), and a computer. The test system could record the time, displacement data, and force data simultaneously. A Teflon plate was installed at the bottom of the sample cell to anchor bubbles. At the same time, the sample cell was placed on an electric lifting

Table 2. Proximate and Ultimate Analyses of the Coal Sample

samples	contact angle θ ($^{\circ}$)	C–C/C–H (%)	C–O (%)	C=O (%)	COOH (%)	wetting heat (J/g)
coal	66.50	70.61	19.90	5.35	4.14	
D + coal	70.58	72.57	18.84	4.61	3.98	–50.66
OA + coal	81.10	73.88	17.87	4.47	3.78	–110.13
OA–D + coal	88.67	74.53	16.60	4.93	3.95	–207.49

platform, which could be moved vertically. Both the micro force balance and the electric lifting platform were controlled by software, and the software could record the displacement data and the force measurement data over time. A high-speed camera was used to record the interaction between the bubble and coal piece. The measurement interval of the micro force balance was 100 ms, and the photo interval of a high-speed camera was 4 ms. A small bubble with a diameter of 4 mm was generated using the micro syringe and placed on the Teflon plate so that it was located directly below the coal piece. To reduce vibration and interference, the whole device was placed on an isolation table and kept at a room temperature of 23 $^{\circ}$ C. The microbalance and force sensor were enclosed in a transparent anti-interference windshield to isolate the influence of the local airflow on the movement of the coal piece and gas–liquid interface.

In the process of force measurement, the coal piece treated with different collectors was adhered to the force sensor. A small bubble was blown at the bottom of the Teflon plate in the sample cell containing deionized water. The lifting platform was moved upward so that the coal piece was immersed into the sample cell, keeping the centerline of the bubble and coal piece aligned. Then, the lifting platform was further moved upward, and the bubble gradually approached the coal piece until the contact and adhesion occurred. After 4 s, the lifting platform was moved down, and the bubble was gradually stretched until it detached from the coal piece and the sample cell was returned to its original position. The movement speed of the lifting platform was 1 mm per second. The force and displacement were recorded synchronously by the software to obtain the force–displacement curve, which was manually integrated to obtain the energy of air bubble detachment from the LRC surface.

3. RESULTS AND DISCUSSION

3.1. Effect of Collectors on LRC Surface Properties. The contact angle, functional group change, and wetting heat of the coal surface treated with different reagents are presented in Table 2. The results show that the contact angle of the coal sample after reagent treatment is increased in the order of OA–D > OA > D. After the treatment with collectors, the coal surface becomes more hydrophobic and homogeneous, and mixed collector OA–D shows better performance than the single collector.

The major combination form of the carbon structure, C–C/C–H, accounts for 70.61%. The contents of oxygen-containing groups, namely, C–O, C=O, and COOH, are 19.90, 5.35, and 4.14%, respectively. After OA–D treatment, the content of C–C/C–H increases by 3.92%, while the contents of C–O, C=O, and COOH decreased by 3.3, 0.42, and 0.19%, respectively. However, the content of C–C/C–H increases by only 1.96 and 3.27% in the cases of D and OA, respectively. It is indicated that OA can form a hydrogen bond with the oxygen-containing groups on the LRC surface. Meanwhile, the polar head of OA mainly bonds with the C–O group and the nonpolar head extends outward. This bridging effect of OA promotes the

adsorption of D in the hydrophobic region or OA-modified region, which shows a synergistic effect between OA and D.

The heat released in the process of the collectors wetting the coal surface is called wetting heat, which is often used to characterize the adsorption intensity of collectors. The wetting heat value is shown in Table 2. It can be seen that the values of the wetting heat are all negative, indicating that the adsorption process of collectors on the coal surface is exothermic and spontaneous. The wetting heat of OA–D is -207.14 g/J, which is almost 2 times that of OA and 4 times that of D. The greater the absolute value of wetting heat, the higher the adsorption intensity of the collector on the coal surface. It is easier for OA–D to wet the coal surface, which may be attributed to the strong force between OA–D and the coal surface, including hydrogen bonding and van der Waals forces. Thus, it can be found that compared with OA and D, OA–D can adsorb more strongly on the coal surface and improve the hydrophobicity more effectively.

3.2. Energy Feature of Air Bubble Detachment from the LRC Surface. The change curve of force with time is shown in Figure 3. First, the bubble moves upward from the initial

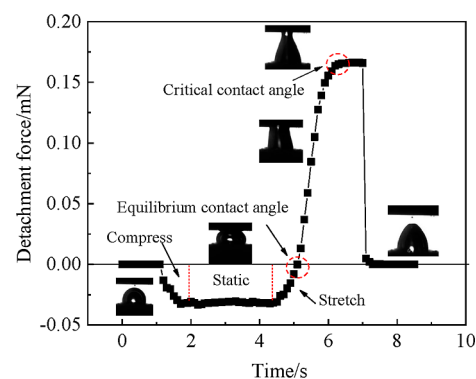


Figure 3. Change curve of the force with time in the detachment force test.

position and approaches the coal surface. The force remains zero until the bubble contacts the coal piece, and it becomes negative after contact. As the bubble continues to move upward, the bubble is compressed, and the absolute value of the force gradually increases. Next, the bubble stops moving upward and stays still. The bubble is in the squeezed state, and the absolute value of the force reaches the maximum and remains unchanged. After that, the bubble moves down and detaches from the coal surface.

This detachment process can be divided into three stages: the relaxation stage, the stretching stage, and the sliding stage.²⁸ The process of the bubble going from the compression state to the equilibrium state is defined as the relaxation stage, during which the force gradually changes from negative to zero. During the stretching stage, the bubble is not detached from the coal surface, and the force becomes positive and gradually increases to the maximum value, which is defined as the detachment force.

During the sliding stage, bubble gradually separates from the coal surface, and the detachment force remain unchanged until the bubble completely detaches from the coal surface. Obviously, the stretching stage and sliding stage constitute the actual detachment process.

Taking the position corresponding to zero detachment force as the starting point of displacement, the change curve of the detachment force with bubble displacement is obtained, as shown in Figure 4. It can be seen that the trend of detachment

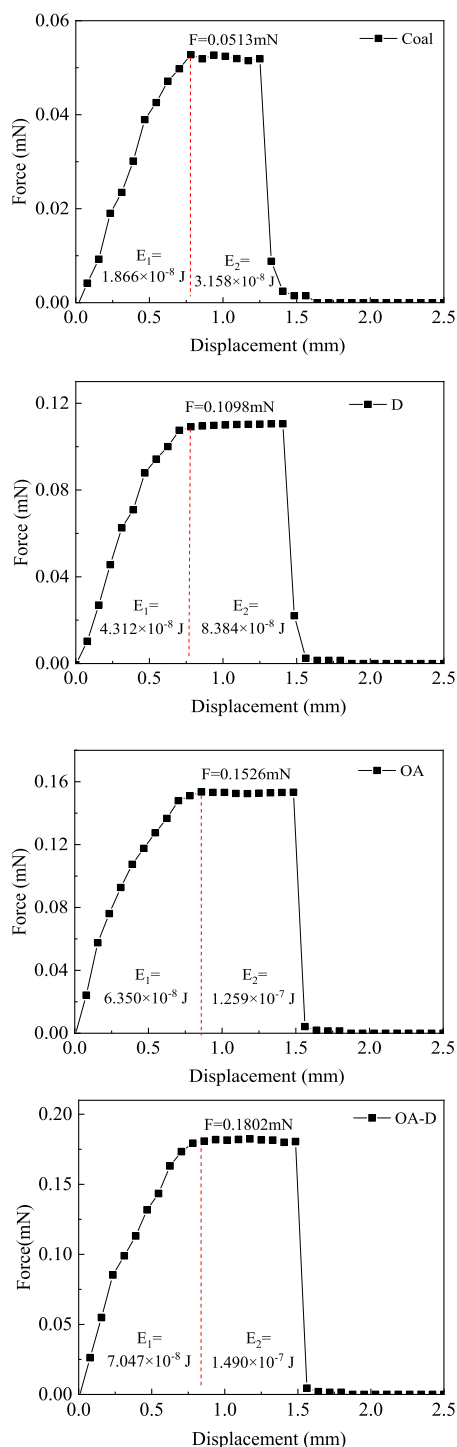


Figure 4. Change curve of the force with bubble displacement in the detachment process.

force changing with bubble displacement is similar to that obtained when the bubble is detached from the LRC surface treated by different collectors, which can be divided into the stretching stage and sliding stage. During the stretching stage, the detachment force gradually increases to the maximum with the increase of bubble displacement. Then, it enters the sliding stage, during which the detachment force remains unchanged until the bubble completely detaches, and the detachment force instantly becomes zero.

On the other hand, the maximum detachment force of the bubble from the LRC surface treated by collectors is obviously different, which increases in the order of coal < D < OA < OA–D. At the same time, the bubble displacement corresponding to the maximum detachment force is different, whose order is the same as that of the detachment force. It can be found that the adhesion strength between bubbles and the LRC surface is improved after the collector treatment. The LRC surface treated by mixed collector OA–D delivers the maximum detachment force and bubble displacement, indicating that the adhesion strength and stability between the bubble and LRC surface treated by OA–D is the highest.

By integrating the detachment force–bubble displacement curve, the detachment energy of the bubble from the LRC surface is obtained. As can be seen from Figure 4, the detachment energy can also be divided into E_1 and E_2 stages. During the detachment test, the bubble is pulled downward and detached from the LRC surface, and the external force overcomes the adhesion to do work. Detachment can only occur when the work done by the external force is equal to or greater than the detachment energy.

It is easy to observe that E_1 and E_2 correspond to the stretching stage and sliding stage during bubble detachment from the LRC surface, respectively. During the stretching stage, the length of the three-phase contact line remains unchanged and the bubble is stretched. When the contact angle reaches the critical contact angle, the bubble starts to slip from the LRC surface, and the force reaches the maximum value, that is, the detachment force. The work done by the external force at this stage is defined as the activation energy E_1 , which is the energy barrier inducing detachment, namely, the energy consumption necessary for the bubble to begin detachment. During the sliding stage, the length of the three-phase contact line is gradually shortened, but the force remains unchanged until the bubble completely detaches from the LRC surface. The work done by the external force at this stage is detachment work, E_2 , which is the actual energy consumption for bubble detachment.

3.3. Theoretical Model of Detachment Energy. Since the detachment work E_2 is the actual energy consumption of bubble detachment and the adhesion work reflects the change of free energy of the system before and after the bubble adhesion to the coal surface, the relationship between detachment work E_2 and adhesion work can be compared. Kim et al.²⁷ proposed that adhesion work is the change of surface free energy during wetting.

In order to calculate the adhesion work of the bubble wetting the coal surface, it is assumed that the coal piece is an ideal surface with no contact angle hysteresis, and the bubble is a sphere and a spherical cap in the initial and final states, respectively, as shown in Figure 5. There is no mass transfer among air bubble, water, water vapor, and coal. The volume of each subject is conserved. At the same time, the influence of line tension, volume force, electromagnetic force, and penetration into the coal piece is ignored, and all properties before and after

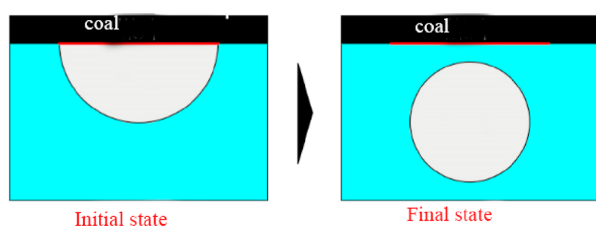


Figure 5. Initial and final states of bubble detachment from the coal surface.

adhesion are considered to be consistent. Based on the above assumptions, the conservation equations and interface constraints are used to establish the following equation

$$\text{mass conservation: } \rho V_1 = \rho V_2 \quad (1)$$

$$\text{Young equation: } \sigma_{sg} - \sigma_{sl} = \sigma_{lg} \cos \theta_e \quad (2)$$

$$\begin{aligned} \text{energy conservation: } & (\sigma_{lg} A_{lg,1} + \sigma_{sl} A_{sl,1}) + w \cdot A_{sg,1} \\ & = \sigma_{lg} A_{lg,2} + \sigma_{sl} A_{sl,2} \end{aligned} \quad (3)$$

where ρ is the air density, V_1 and V_2 are the initial and final state volumes, respectively; σ_{sg} , σ_{sl} , and σ_{lg} are the tension values at the solid–air interface, solid–liquid interface, and liquid–air interface, respectively; θ_e is the equilibrium contact angle; $A_{ld,1}$, $A_{sl,1}$, and $A_{sg,1}$, respectively correspond to the liquid–gas interface, solid–liquid interface, and solid–gas interface contact areas in the initial state; $A_{lg,2}$ and $A_{sl,2}$ represent the liquid–gas interface and solid–liquid interface contact areas in the final state, respectively, and w represents the adhesion work per unit solid–gas contact area; and $w \cdot A_{sg,1}$ represents the adhesion work W of the interaction between the bubble and coal surface.

The solid–gas interface contact area of the initial state is equal to the newly added solid–liquid interface contact area of the final state, that is

$$A_{sg,1} = A_{sl,2} \quad (4)$$

Combining the above four formulas, substituting the geometric parameters (Table 3) of the initial state spherical

Table 3. Geometric Parameters of the Spherical Cap and Sphere^a

parameters	sphere	spherical cap
volume (V)	$4/3\pi r^3$	$\pi R^3(2/3 - \cos \theta + 1/3 \cos^3 \theta)$
contact angle area of the liquid–gas interface (A_{lg})	$4\pi r^2$	$2\pi R^2(1 - \cos \theta)$
solid–liquid interface contact angle area (A_{sl})	$\pi(r \sin \theta)^2$	0
contact angle area of the solid–air interface (A_{sg})	0	$\pi(R \sin \theta)^2$

^a r , radius of the spherical bubble and R , radius of the spherical cap.

cap and the final state sphere into the equation, the following equation can be obtained

$$\begin{aligned} w/\sigma_{lg} = & 4((2 - \cos \theta_e)(1 + \cos \theta_e)^2/4)^{2/3} \\ & - 2(1 + \cos \theta_e)/\sin^2 \theta_e - \cos \theta_e \end{aligned} \quad (5)$$

where w/σ_{lg} is the adhesion work per unit gas–liquid interfacial tension.

Based on eq 5 and the integral of the force–displacement curve, the energy feature of bubble detachment from the LRC surface is obtained, as shown in Table 4. It can be seen that the order of activation energy is coal < D < OA < OA–D. The activation energy of the mixed collector OA–D is the highest, and the activation energy is the lowest when no reagent is used. The order detachment work of each collector is the same as that of activation energy. It is worth noting that the detachment work is close to the calculated adhesion work, so it is further proved that E_2 represents the actual energy consumption for bubble detachment.

The E_{total} ($=E_1 + E_2$) is the total work during the whole process of the bubble moving from the equilibrium to complete detachment from the LRC surface. After the collector treatment, the activation energy, detachment work, and total energy between bubbles and the LRC surface all increase significantly. The total energy of each collector shows the same order as that of activation energy and detachment work. The activation energy, detachment work, and total energy of mixed collector OA–D are all greater than those of the the single collector. It is indicated that there is a synergistic effect between OA and D, which increases the adhesion strength and stability between bubble and LRC surface.

This force measurement and energy calculation of bubble detachment from the LRC surface showed that the detachment force and energy of the single reagent was greatly improved by the use of the mixture, and OA and D showed a synergistic effect in suppressing bubble detachment from the LRC surface, which was mainly due to the increase of LRC surface hydrophobicity. The contact angle measurement indicated that the contact angle for coal treated with D, OA, and OA–D was higher than that for untreated coal particles, and the order was OA–D > OA > D. This was mainly because the polar head of OA mainly absorbed on the C–O group of the LRC surface and the nonpolar head extended outward, which facilitated D to absorb on the hydrophobic area of the LRC surface or the area modified by OA.

The hydrophobicity of particles strongly influenced the capillary force that was the dominant force to maintain the stability of the bubble–particle aggregate. The effect of OA–D on LRC surface hydrophobicity improved the adhesion strength and stability between bubbles and the LRC surface so as to reduce the particle detachment probability and increase the flotation recovery. This has been confirmed in our previous flotation test,^{1,11} in which the best flotation result was obtained using OA–D as the collector at the dosage of 3 kg/t, and the

Table 4. Energy Feature of Bubble Detachment from the LRC Surface

name	activation energy E_1 (J)	detachment work E_2 (J)	calculated work of adhesion W (J)	total energy E_{total} (J)
coal	1.866×10^{-8}	3.158×10^{-8}	7.454×10^{-8}	5.024×10^{-8}
D	4.312×10^{-8}	8.384×10^{-8}	9.208×10^{-8}	1.270×10^{-7}
OA	6.350×10^{-8}	1.259×10^{-7}	1.230×10^{-7}	1.894×10^{-7}
OA–D	7.047×10^{-8}	1.490×10^{-7}	1.516×10^{-7}	2.195×10^{-7}

combustible matter recovery was 25.77 and 48.86% higher than that of OA and D, respectively. Therefore, the results of detachment force and energy measurements in this study are consistent with those of hydrophobicity measurement and flotation test.

4. CONCLUSIONS

In this paper, the force and displacement of bubble detachment from the LRC surface treated by D, OA and OA–D was measured, and the energy feature during the whole detachment process was investigated. The main conclusions are as follows:

- (1) After collector treatment, the C–C/C–H content on the LRC surface increased, while the content of oxygen-containing functional groups decreased, which improved the LRC surface hydrophobicity. The polar head of OA formed hydrogen bonds with the oxygen-containing groups on the LRC surface, and the nonpolar head extended outward to promote the adsorption of D in the hydrophobic region or OA-modified region. Compared to OA and D single collectors, the synergistic effect enabled OA–D to release more wetting heat when wetting the LRC surface and to obtain a higher contact angle.
- (2) The actual detachment process of bubbles from the LRC surface was divided into the stretching stage and sliding stage. During the stretching stage, the detachment force gradually increased to the maximum with the increase of bubble displacement. Then, it entered the sliding stage, during which the detachment force remained unchanged until the bubble completely detached, and the detachment force instantly became zero. Both the maximum force and displacement for bubble detachment from the LRC surface treated by different collectors decreased in the order of OA–D > OA > D.
- (3) The total energy of the detachment process was composed of activation energy and detachment work. The detachment work was close to the theoretically calculated adhesion work, indicating that detachment work represented the actual energy consumption for bubble detachment. The activation energy, detachment work, and total energy for bubble detachment from the LRC surface treated by different collectors all decreased in the order of OA–D > OA > D. Mixed collector OA–D had a synergistic effect on the enhancement of the LRC hydrophobicity, and it can significantly improve the adhesion strength and stability between bubbles and the LRC surface.

■ AUTHOR INFORMATION

Corresponding Author

Yinfei Liao – National Engineering Research Center of Coal Preparation and Purification, China University of Mining and Technology, Xuzhou 221116, P.R. China; orcid.org/0000-0003-3992-3139; Phone: +86 15852174496; Email: ruiyin@126.com; Fax: +86 051683885878

Authors

Maoyan An – School of Transportation Engineering and Jiangsu Engineering Lab of Biomass Resources Comprehensive Utilization, Jiangsu Vocational Institute of Architectural Technology, Xuzhou 221116, P.R. China

Zhe Yang – School of Chemical Engineering and Technology, China University of Mining and Technology, Xuzhou 221116, P.R. China

Yijun Cao – National Engineering Research Center of Coal Preparation and Purification, China University of Mining and Technology, Xuzhou 221116, P.R. China

Xiaodong Hao – School of Chemical Engineering and Technology, China University of Mining and Technology, Xuzhou 221116, P.R. China

Xingwei Song – School of Chemical Engineering and Technology, China University of Mining and Technology, Xuzhou 221116, P.R. China

Hourui Ren – School of Chemical Engineering and Technology, China University of Mining and Technology, Xuzhou 221116, P.R. China

Aosheng Yang – School of Chemical Engineering and Technology, China University of Mining and Technology, Xuzhou 221116, P.R. China

Luojian Chen – School of Chemical Engineering and Technology, China University of Mining and Technology, Xuzhou 221116, P.R. China

Complete contact information is available at:

<https://pubs.acs.org/10.1021/acsomega.2c00453>

Notes

The authors declare no competing financial interest.

■ ACKNOWLEDGMENTS

This work was supported by the Social Development Key R&D Program of Xuzhou (KC21285), Science Foundation of Jiangsu Province (BK20211048), National Natural Science Foundation of China (52004283), and Natural and National Key R&D Program of China (2020YFC1908803).

■ REFERENCES

- (1) Liao, Y.; Hao, X.; An, M.; Yang, Z.; Ma, L.; Ren, H. Enhancing low-rank coal flotation using mixed collector of dodecane and oleic acid: Effect of droplet dispersion and its interaction with coal particle. *Fuel* **2020**, *280*, 118634.
- (2) Yang, Z.; Xia, Y.; Guo, F.; Xing, Y.; Gui, X. Interaction characteristics between diesel and coal with different hydrophilicity: Kinetic and force effects. *Sep. Purif. Technol.* **2020**, *232*, 115958.
- (3) Xia, Y.; Xing, Y.; Gui, X. Oily collector pre-dispersion for enhanced surface adsorption during fine low-rank coal flotation. *J. Ind. Eng. Chem.* **2020**, *82*, 303–308.
- (4) Zhang, L.; Sun, X.; Li, B.; Xie, Z.; Guo, J.; Liu, S. Experimental and molecular dynamics simulation study on the enhancement of low rank coal flotation by mixed collector. *Fuel* **2020**, *266*, 117046.
- (5) Jia, R.; Harris, G. H.; Fuerstenau, D. W. An improved class of universal collectors for the flotation of oxidized and/or low-rank coal. *Int. J. Miner. Process.* **2000**, *58*, 99–118.
- (6) Tian, Q.; Zhang, Y.; Li, G.; Wang, Y. Application of carboxylic acid in low-rank coal flotation. *Int. J. Coal Prep. Util.* **2019**, *39*, 44–53.
- (7) Zhang, R.; Xing, Y.; Xia, Y.; Guo, F.; Ding, S.; Tan, J.; Che, T.; Meng, F.; Gui, X. Synergistic adsorption mechanism of anionic and cationic surfactant mixtures on low-rank coal flotation. *ACS Omega* **2020**, *5*, 20630–20637.
- (8) Jia, R.; Harris, G. H.; Fuerstenau, D. W. Chemical reagents for enhanced coal flotation. *Coal Prep.* **2002**, *22*, 123–149.
- (9) Zhen, K.; Zhang, H.; Zheng, C. Wettability modification and flotation intensification of low-rank coal with dodecyl trimethyl ammonium chloride addition. *J. Therm. Anal. Calorim.* **2019**, *137*, 2007–2016.
- (10) Liu, Z.; Xia, Y.; Lai, Q.; An, M.; Liao, Y.; Wang, Y. Adsorption behavior of mixed dodecane/n-valeric acid collectors on low-rank coal

surface: Experimental and molecular dynamics simulation study. *Colloids Surf., A* **2019**, *583*, 123840.

(11) An, M.; Liao, Y.; Cao, Y.; Hao, X.; Ma, L. Improving low rank coal flotation using a mixture of oleic acid and dodecane as collector: A new perspective on synergetic effect. *Processes* **2021**, *9*, 404.

(12) Matveeva, T. N.; Gromova, N. K.; Lantsova, L. B. Adsorption of tannin-bearing organic reagents on stibnite, arsenopyrite and chalcopyrite in complex gold ore flotation. *J. Min. Sci.* **2016**, *52*, 551–558.

(13) Wang, G.; Nguyen, A. V.; Mitra, S.; Joshi, J. B.; Jameson, G. J.; Evans, G. M. A review of the mechanisms and models of bubble-particle detachment in froth flotation. *Sep. Purif. Technol.* **2016**, *170*, 155–172.

(14) Bournival, G.; Ata, S.; Jameson, G. J. Bubble and froth stabilizing agents in froth flotation. *Miner. Process. Extr. Metall. Rev.* **2017**, *38*, 366–387.

(15) Nutt, C. W. Froth flotation: The adhesion of solid particles to flat interfaces and bubbles. *Chem. Eng. Sci.* **1960**, *12*, 133–141.

(16) Schulze, H. J. New theoretical and experimental investigations on stability of bubble/particle aggregates in flotation: a theory on the upper particle size of floatability. *Int. J. Miner. Process.* **1977**, *4*, 241–259.

(17) Zhang, Y.; Xing, Y.; Ding, S.; Cao, Y.; Gui, X. Effect of vibration mode on detachment of low-rank coal particle from oscillating bubble. *Powder Technol.* **2019**, *356*, 880–883.

(18) Kondrat'ev, S. A. Influence of main flotation parameters on detachment of hydrophilic particle from bubble. *J. Min. Sci.* **2005**, *41*, 373–379.

(19) Fosu, S.; Skinner, W.; Zanin, M. Detachment of coarse composite sphalerite particles from bubbles in flotation: Influence of xanthate collector type and concentration. *Miner. Eng.* **2015**, *71*, 73–84.

(20) Wang, P.; Reyes, F.; Cilliers, J. J.; Brito-Parada, P. R. Evaluation of collector performance at the bubble-particle scale. *Miner. Eng.* **2020**, *147*, 106140.

(21) Zhu, C.; Xing, Y.; Xia, Y.; Wang, Y.; Li, G.; Gui, X. Flotation intensification of low-rank coal using a new compound collector. *Powder Technol.* **2020**, *370*, 197–205.

(22) Li, M.; Xia, Y.; Zhang, Y.; Ding, S.; Rong, G.; Cao, Y.; Xing, Y.; Gui, X. Mechanism of shale oil as an effective collector for oxidized coal flotation: From bubble–particle attachment and detachment point of view. *Fuel* **2019**, *255*, 115885.

(23) Chen, S.; Yang, Z.; Chen, L.; Tao, X.; Tang, L.; He, H. Wetting thermodynamics of low rank coal and attachment in flotation. *Fuel* **2017**, *207*, 214–225.

(24) Ren, H.; Liao, Y.; Yang, Z.; An, M.; Hao, X.; Song, X.; Liu, Z. Effect of Fe²⁺ on low rank coal flotation using oleic acid as collector. *Powder Technol.* **2021**, *393*, 250–256.

(25) Yang, Z.; Liao, Y.; Ren, H.; Hao, X.; Song, X.; Liu, Z. A novel co-treatment scheme for waste motor oil and low rank coal slime: Waste dispose waste. *Fuel* **2021**, *292*, 120275.

(26) Liao, Y.; Yang, Z.; An, M.; Cao, Y.; Hao, X.; Song, X.; Ren, H.; Yang, A.; Chen, L. Spreading behavior of dodecane-oleic acid collector mixture in low-rank coal flotation. *Fuel* **2022**, *308*, 122071.

(27) Liao, Y.; Ren, H.; An, M.; Cao, Y.; Yang, Z.; Hao, X.; Song, X. Detachment force of air bubbles detached from low-rank coal surface in the presence of adsorbed oleic acid–dodecane collector mixture. *ACS Omega* **2021**, *6*, 7746–7753.

(28) Liao, Y.; Ren, H.; An, M.; Cao, Y.; Ma, L.; Hao, X.; Liu, Z.; Yang, Z. Kinetics of bubble interaction with low rank coal surface in the presence of adsorbed dodecane-oleic acid collector mixture. *Minerals* **2021**, *11*, 1–14.

(29) Kim, S. H.; Park, H. S.; Ko, D.; Kim, M. H. Wetting characteristic of bubble on micro-pillar structured surface under a water pool. *Exp. Therm. Fluid Sci.* **2019**, *100*, 135–143.